Photochemistry and Photobiology, 2017, 93: 1430–1438

^{31}P NMR Evidence for Peroxide Intermediates in Lipid Emulsion Photooxidations: Phosphine Substituent Effects in Trapping

Prabhu P. Mohapatra[1], Callistus O. Chiemezie[1,2], Arina Kligman[1,2], Michele M. Kim[3,4], Theresa M. Busch[3], Timothy C. Zhu[3] and Alexander Greer[1,2]*

[1]Department of Chemistry, Brooklyn College, Brooklyn, NY
[2]Ph.D. Program in Chemistry, The Graduate Center of the City University of New York, New York, NY
[3]Department of Radiation Oncology, University of Pennsylvania, Perelman Center for Advanced Medicine, Philadelphia, PA
[4]Department of Physics and Astronomy, University of Pennsylvania, Philadelphia, PA

Received 10 May 2017, accepted 26 June 2017, DOI: 10.1111/php.12810

ABSTRACT

Intralipid is a lipid emulsion used in photodynamic therapy (PDT) for its light scattering and tissue-simulating properties. The purpose of this study is to determine whether or not Intralipid undergoes photooxidation, and we have carried out an Intralipid peroxide trapping study using a series of phosphines [2′-dicyclohexylphosphino-2,6-dimethoxy-1,1′-biphenyl-3-sulfonate, 3-(diphenylphosphino)benzenesulfonate, triphenylphosphine-3,3′,3″-trisulfonate and triphenylphosphine]. Our new findings are as follows: (1) An oxygen atom is transferred from Intralipid peroxide to the phosphine traps in the dark, after the photooxidation of Intralipid. 3-(Diphenylphosphino)benzenesulfonate is the most suitable trap in the series owing to a balance of nucleophilicity and water solubility. (2) Phosphine trapping and monitoring by ^{31}P NMR are effective in quantifying the peroxides in H_2O. An advantage of the technique is that peroxides are detected in H_2O; deuterated NMR solvents are not required. (3) The percent yield of the peroxides increased linearly with the increase in fluence from 45 to 180 J cm^{-2} based on our trapping experiments. (4) The photooxidation yields quantitated by the phosphines and ^{31}P NMR are supported by the direct ^{1}H NMR detection using deuterated NMR solvents. These data provide the first steps in the development of Intralipid peroxide quantitation after PDT using phosphine trapping and ^{31}P NMR spectroscopy.

INTRODUCTION

The phosphine trapping of fatty acid ester hydroperoxides formed from Intralipid® photooxidations and monitoring by ^{31}P NMR spectroscopy is a potentially novel, but untested process (Fig. 1).

Because of the use of Intralipid in photodynamic therapy (PDT) (1–3) and its tissue-simulating properties (4–10), there is interest in the reactivity of its alkene bonds with reactive oxygen species (ROS), particularly singlet oxygen ($^{1}O_2$). Current knowledge of $^{1}O_2$ reactivity is limited to constituents of such as the individual fatty acids and alkenes, and membranes (11–26) rather than the Intralipid emulsions themselves. Intralipid emulsions consist of soybean oil alkenes and polyenes, egg yolk phospholipids, glycerin and water.

Previous PDT studies on Intralipid have mainly focused on $^{1}O_2$ luminescence (27). In a recent advance in this field, Gemmell *et al.* (27) identified a decrease of $^{1}O_2$ luminescence in Intralipid fluid, however, it is not known whether it was due to $^{1}O_2$ quenching, other de-excitation pathways, and/or diffusion of excitation and $^{1}O_2$ luminescence at 1270 nm. The photosensitizer concentration in tissue as measured during pleural PDT varies from 0 to 20 μM and depends on the degree of heterogeneities, with a mean of around 5.9 μM (28). As a result of surgery and/or PDT, the photosensitizer that is circulating can leak into the Intralipid. For pleural PDT, Intralipid will fill the chest cavity (29,30). As a result, the amount of photosensitizer that could leak into the Intralipid will be less than 20 μM after dilution by the Intralipid solution in the pleural cavity. For experimental convenience, 100 μM AlPcS (photosensitizer) is used in many of our experiments.

Thus, there is a need to develop chemical trapping methods and spectroscopic techniques for quantifying the amount of fatty acid ester hydroperoxides in Intralipid photooxidation samples. Our hypothesis is that irradiation of Intralipid in the presence of O_2 and a sensitizer will form peroxy species that can be trapped. Our approach includes a combination of organic trapping chemistry, photochemistry and NMR spectroscopy. Here, organic photochemistry and NMR methods were used to reveal the photooxidative instability of Intralipid.

The potential for *O*-atom trapping of photooxidized Intralipid samples is yet unexplored. We envisioned that Intralipid photoperoxides likely exist because membrane photoperoxides exist (11–19). We sought to develop an Intralipid peroxide trapping process. The issues addressed in this report are the light fluence dependence of the process and phosphine substituent effects.

Here, our strategy involved the use of four phosphines [sSPhos (2′-dicyclohexylphosphino-2,6-dimethoxy-1,1′-biphenyl-3-sulfonate (**1**), 3-(diphenylphosphino)benzenesulfonate ion (**2**), triphenylphosphine-3,3′,3″-trisulfonate ion (**3**) and triphenylphosphine (**4**)] in our peroxide trapping studies (Fig. 2). These phosphines vary in the number of aliphatic and aromatic substituents, and the number of water-solubilizing sulfonate groups. sSPhos is

*Corresponding author email: agreer@brooklyn.cuny.edu (Alexander Greer)

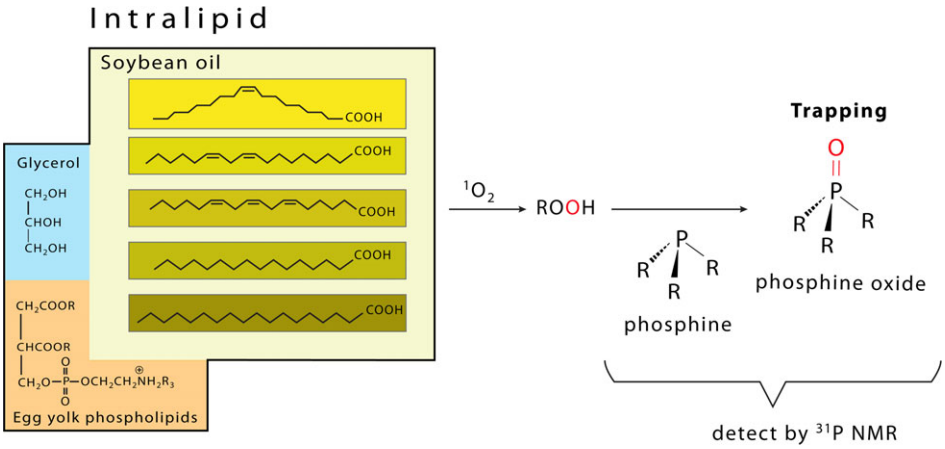

Figure 1. Photooxidation of Intralipid and monitoring of the resulting hydroperoxides by ^{31}P NMR spectroscopy.

unique; it contains two cyclohexane rings and an arylsulfonate ion. Bulky electron-rich phosphines such as sSPhos **1** are ligands for Suzuki–Miyaura cross-coupling reactions in the field of organic synthesis, facilitating C–C, C–N and C–O bond formations (31–36). Organic solvent soluble phosphines are highly oxophilic and trap oxygen from peroxide sources (37–44). These processes include phosphorus biphilic insertion to obtain phosphorane intermediates (45–47). Water-soluble phosphines such as **3** have been used to prepare gold complexes as catalysts (48), but not as trapping agents in aqueous reactions during PDT.

Here, we report that an oxygen atom is diverted from Intralipid peroxides to phosphines **1**–**4**, but with different efficiencies. Our phosphine trapping observation is consistent with direct ^{1}H NMR data on hydroperoxides using deuterated solvents. However, a facet of this study is that deuterated solvents are not required to monitor the trapping by ^{31}P NMR so that aqueous samples are readily usable. Our work builds on previous reports of phosphine trapping as *in situ* trapping agents for heteroatom and hydrocarbon peroxides, but in a model reaction for PDT.

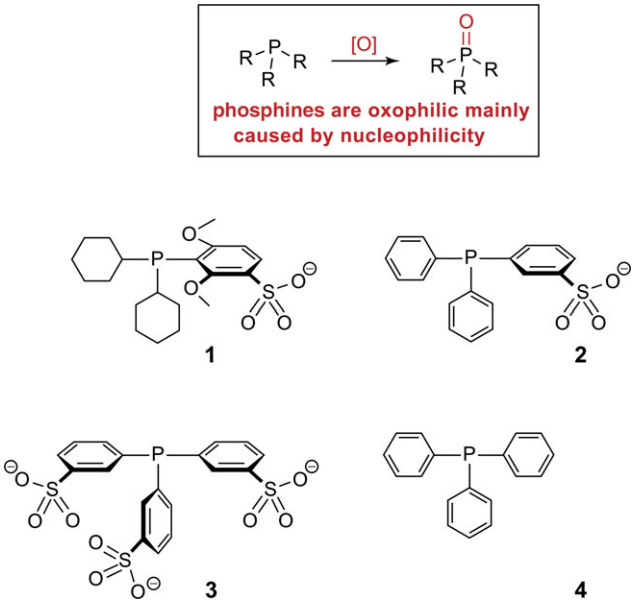

Figure 2. The four phosphines (**1**–**4**) used in our peroxide trapping studies, which upon oxidation form the corresponding phosphine oxides.

MATERIALS AND METHODS

Reagents and instrumentation. AlPcS, oleic acid, soybean oil, phosphines **1**–**4**, $K_2Cr_2O_7$, $CDCl_3$ and CD_3OD were purchased commercially and used as received without further purification. Intralipid fluid was diluted to 1% (v/v) from a 20% emulsion of soybean oil (10%), egg yolk phospholipids (1.2%), glycerin (2.25%) and water. Soybean oil consists of linoleic acid (44–62%), oleic acid (19–30%), palmitic acid (7–14%) and linolenic acid (4–11%). ^{1}H NMR spectra were acquired at 400 MHz, and ^{31}P NMR spectra were acquired at 161.9 MHz using a Bruker DPX400 MHz instrument.

Photogeneration of singlet oxygen. Two photooxidation methods were used as follows: (1) Intralipid (1% aqueous solution) and sensitizer AlPcS (1×10^{-4} M) in 0.6 mL H_2O were irradiated with a diode laser (669 nm light through a fiber, power density = 0.2 W cm^{-2} and fluences ranging from 45 to 180 J cm^{-2}). The fiber optic was situated above a $1 \times 1 \times 1$ cm^3 cuvette containing 0.6 mL solution sitting on the detector. Thus, the diode laser light was specified as in-air light fluence because of the geometry (light is incident from the top and passes through 0.6 cm thick material). In an optical phantom that involves scattering and attenuation materials, the light longitudinal attenuation can be expressed as $\exp(-\mu_{eff} \times \text{depth})$ ~0.8, where μ_{eff} is the inverse of the optical penetration depth = sqrt $(3 \times \mu_a \times \mu_s') = 0.39$ cm^{-1} (49,50). In this expression, μ_s' is the reduced scattering coefficient and μ_a is the absorption coefficient. In the near-infrared (NIR) region, the scattering coefficient is always much larger than the absorption coefficient. As a result, the effective attenuation coefficient is determined by a combination of scattering and absorption coefficient (49,50). (2) Samples of soybean oil (50 mM) or oleic acid (50 mM) and sensitizer AlPcS (0.1 mM) in 0.6 mL $CDCl_3$ or CD_3OD were irradiated with two 400 W metal halide lamps through a 0.05 M $K_2Cr_2O_7$ solution in 0.5% v/v H_2SO_4 cutoff filter ($\lambda > 500$ nm) solution. Using a calibrated isotropic detector connected to a custom dosimetry system, the fluence rate at the location between the two bulbs (separated by 14.5 cm) where the sample was located was found to be 21.8 ± 2.4 mW cm^{-2}. The fluence rate at various locations around the metal halide lamp with a power meter for two distances from the bulb (5 and 10 cm) is shown in Fig. 3. Prior to the irradiation, both methods included O_2 bubbling in the solutions for 6 min at a slow bubble-by-bubble rate.

Peroxide trapping reactions with phosphine. After the irradiation, **1**–**4** (40 μmol, 1 equiv) was added to the reaction mixture and analyzed by ^{31}P NMR spectroscopy (Figures S2–S4). The hydroperoxide yields were reproducible. The following parameters were used in acquiring the ^{31}P NMR spectra for our trapping study: the acquisition time was 0.51 s, the number of scans was 300, the spectral width was 64102.563 Hz, the pulse delay was 7.32 μs, the pulse width was 61 W and the total number of data points was 65536.

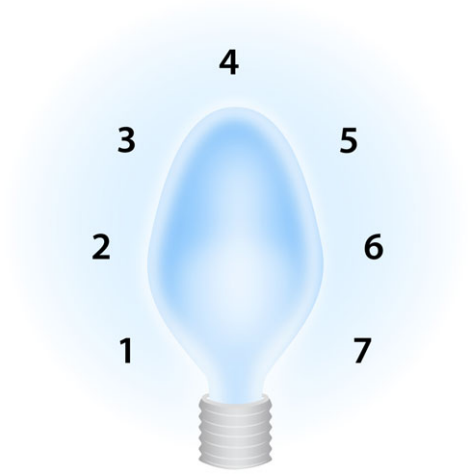

Location	Fluence Rate ($mW\ cm^{-2}$) at 5 cm	Fluence Rate ($mW\ cm^{-2}$) at 10 cm
1	14.8 ± 0.5	7.3 ± 1.4
2	20.6 ± 3.5	7.2 ± 0.5
3	12.7 ± 5.3	62.5 ± 4.4
4	1.4 ± 1.1	0.7 ± 0.3
5	9.7 ± 3.2	4.3 ± 3.5
6	20.4 ± 9.0	11.3 ± 3.5
7	15.3 ± 0.3	8.8 ± 3.0

Figure 3. The measured fluence rate of the metal halide lamp.

Intralipid peroxides. Peroxides were formed in H_2O containing AlPcS (0.1 mM) and Intralipid (9 mM oleic acid, 19 mM linoleic acid, 3 mM linolenic acid, 4 mM palmitic acid, 1 mM stearic acid, 10 mM glycerol and 0.6 mM egg yolk phospholipids). Oxygen was bubbled for 6 min, and the sample was irradiated from above with a 669 nm diode laser.

Soybean oil peroxides. Several peroxide products were formed in 0.6 mL $CDCl_3$ or CD_3OD containing AlPcS (0.1 mM) and soybean oil (8 mM oleic acid, 20 mM linoleic acid, 2 mM linolenic acid, 4 mM palmitic acid and 1 mM stearic acid). Oxygen was bubbled for 6 min, and the sample was irradiated with a pair of metal halide lamps through the $K_2Cr_2O_7$ cutoff filter solution.

Oleic acid peroxides. Regioisomeric hydroperoxides were formed in 0.6 mL CD_3OD containing AlPcS (0.1 mM) and oleic acid (40 mM). Oxygen was bubbled for 6 min, and the sample was irradiated with a pair of metal halide lamps through the $K_2Cr_2O_7$ cutoff filter solution. ^1H NMR 400 MHz ($CDCl_3$): 0.92 (t, J = 6.4 Hz, 3H), 1.35–1.31 (m, 20H), 1.61 (t, 7.2 Hz, 3H), 2.10–2.03 (m, 4H), 2.29 (t, J = 15.2 Hz, 2H), 4.18 (q, J = 6 Hz, 1H, OC<u>H</u> protons of peroxides), 5.41–5.32 (m, 2H), 5.73–5.66 (m, 2H, olefinic protons of peroxides).

RESULTS AND DISCUSSION

Four phosphines (**1**–**4**) were used in our peroxide trapping studies.

Apparatus

A laser setup with a cuvette containing Intralipid was used as a model for irradiation in the pleural cavity (Fig. 4). The apparatus delivers 669 nm light to the air/water interface (fluence rate 0.2 W cm^{-2}; fluences: 45, 90, 135 and 180 J cm^{-2}). For preparative scales to facilitate the characterization of products by NMR, a pair of metal halide lamps was used (fluence rate of 21.8 mW cm^{-2}), filtered in the wavelength range of 500–700 nm as described in the Experimental Section. As we will see, the O trapping occurs in the dark via the trapping of peroxides with phosphines after the photoreactions, but in one case for **1**, O-atom transfer reactions also occurred by air oxidation.

Phosphine stability and solubility

Addition of a phosphine (**1**–**4**) to Intralipid alone (without photooxidation/photoreaction) did not result in the formation of the corresponding phosphine oxide. When reactions were carried out in the dark in O_2-saturated H_2O, the O-atom transfer was not observed in phosphines **2**–**4**. However, the reaction of sSPhos **1** in the dark and in the presence of air showed O-atom transfer. Air, but not water, was found to be the source of the O atom in **1** oxide. Consequently, the phosphine trapping approach with sSPhos **1** required a correction factor as the total **1** oxide formed included quantities from peroxides and air oxidation of **1** as we will see below.

As reported in the literature, alkyl substituted phosphines are susceptible to air oxidation (51–53). Phosphine **2** produced <1% of the corresponding phosphine oxide by bubbling O_2 in D_2O or CD_3OD. Experiments showed that the yield of **4** oxide was poor due to the lack of solubility in the aqueous Intralipid media. This is in contrast to the case of **3** in the phosphine series, which was inefficient in trapping peroxides. Phosphine **3** is capable of trapping peroxy species, but it is slow and relatively unreactive to peroxy species and the peroxides generated in Intralipid photooxidation reactions. Control experiments showed that the yield of **3** oxide was about three-fold to four-fold less in the photoreaction of Intralipid with O_2 compared to phosphine **2** after 15 min. The poor peroxide reactivity of **3** can be attributed to the presence of three sulfonate groups (electron-withdrawing substituents), making the phosphorus site a relatively poor nucleophile. The O trapping plateaued with time; that is the Intralipid peroxides reacted with phosphines **1** and **2** rapidly after the experiments were performed. Notably, some peroxides probably decomposed before we could trap them with phosphines. Thus, the reported values of O trapping in this study can be considered as the lower limit.

Detecting peroxides with trapping and ^{31}P NMR

The 669 nm light irradiation of Al(III) phthalocyanine tetrasulfonate (AlPcS) sensitizer in the presence of Intralipid and O_2 led to the formation of peroxides. The concentration of peroxide was monitored by the disappearance of sSPhos **1** (−8.20 ppm) and the appearance of **1** oxide (55.98 ppm) (Fig. 5). The peroxide yields were obtained as a function of light fluence (Table 1). Table 1 shows the trapping data of Intralipid peroxides using phosphines **1**–**3** in the fluence range 45–180 J cm^{-2}. In the case of 100 μM AlPcS, a fluence of 90 J cm^{-2} led to 9.3% Intralipid oxidation, where 4.1 mM peroxide was detected by a photooxidation trapping reaction by sSPhos **1** of a sample containing 44 mM Intralipid. Table 1 shows that the O-atom transfer was dependent on the fluence, but less so on the concentration of the sensitizer, that is the yield of **1** oxide and **2** oxide increased from ~8% to ~17% when the fluence was increased from 45 to 180 J cm^{-2}. At 90 J cm^{-2},

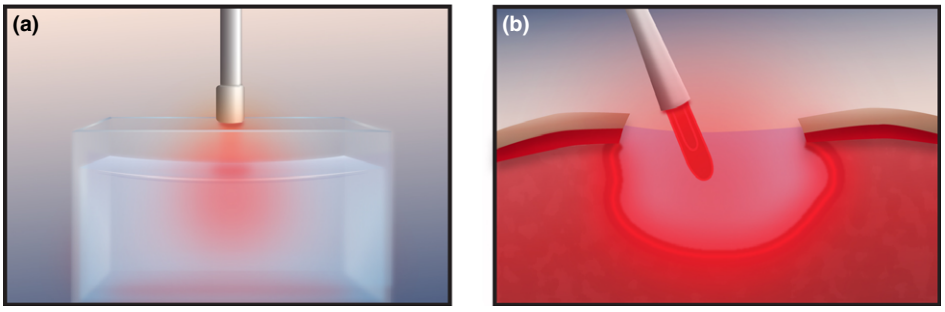

Figure 4. Model for irradiation of Intralipid in the pleural cavity. (a) Image of the laser setup with a cuvette. The apparatus delivers 669 nm light to the air/water interface. The solution in the cuvette is 1% Intralipid and contains 0.1 mM Al(III) phthalocyanine tetrasulfonate ion (AlPcS) sensitizer. The red light is shined from above, where the air-gap distance from the fiber-optic cable to the water surface in the middle of meniscus in the cuvette is 5 cm. (b) Image of laser irradiation in the pleural cavity.

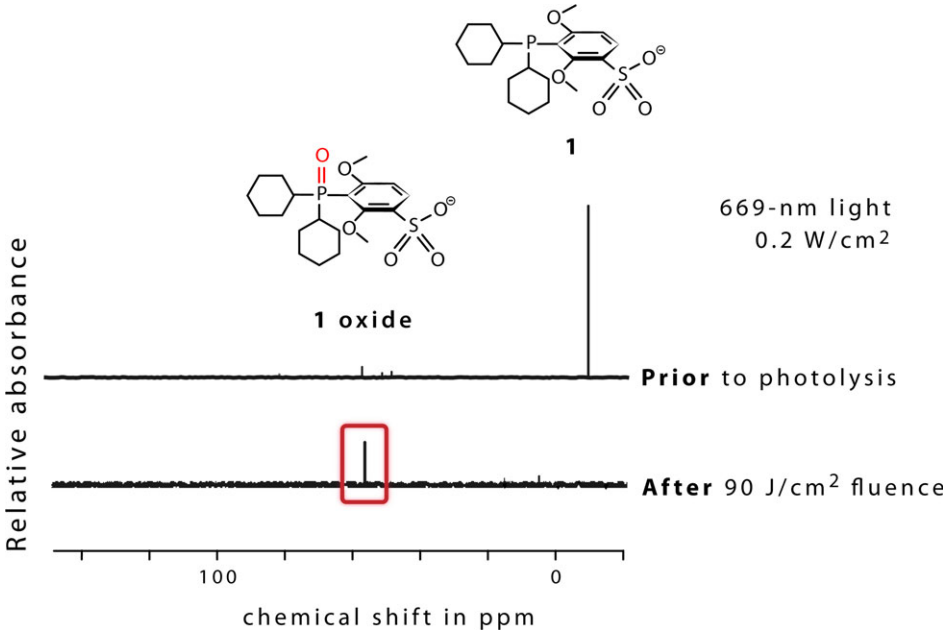

Figure 5. The detection of peroxides by sSPhos **1** in the dark using ^{31}P NMR spectroscopy. For **1**, as little as ~0.5 mM of peroxides is detectable.

the percent yield of **2** oxide decreased from 9.3% to 5% with decreasing AlPcS concentration from 100 μM to 10 nM. Photoactivity of sensitizers in nanomolar quantities is of interest in the field of PDT (54–59), and while our data show 5% photooxidation at 10 nM concentrations of AlPcS, effects such as the location of the sensitizer in Intralipid were not assessed.

Detecting peroxides with ^{1}H NMR

The suggestion of Intralipid peroxide formation by ^{31}P NMR with phosphine trapping is supported by the ^{1}H NMR data obtained for similar reactions (Fig. 6). The formation of hydroperoxides is evident from the ^{1}H NMR spectra of soybean oil and oleic acid photooxidation reactions shown in Figs. 7 and 8. Figure 7 shows one regioisomeric hydroperoxide formed by the photooxidation of a triglyceride of linoleic acid, a constituent of soybean oil. It is common that fatty acids in soybean oil are not in the free form, but are esterified to the corresponding triglycerides in the presence of glycerol and plant enzymes.

Table 1. Trapping of peroxides by phosphines 1–4 from 1% (v/v) Intralipid* photooxidations

Entry	Fluence (J cm^{-2})	Irrad. time (min)	[sens]†	Peroxide yield (%) 1	2	3	4
1	45	3.75	1×10^{-4} M	9 ± 1.5	8.3 ± 1		
2	90	7.5	1×10^{-4} M	10 ± 1.5	9.3 ± 1		
3	135	11.25	1×10^{-4} M	13	13 ± 1		
4	180	15	1×10^{-4} M	18 ± 1.5	17 ± 1	2	–
5	90	7.5	1×10^{-6} M		7 ± 1		
6	90	7.5	1×10^{-8} M		5 ± 1		

*1% (v/v) Intralipid = 44 mM. †Sensitizer is AlPcS.

The formation of hydroperoxides was also observed by ^{1}H NMR studies in the photooxidation of oleic acid (Fig. 8). Figure 8 shows the structural assignment of one of the two regioisomeric hydroperoxides formed in the photooxidation of oleic acid. The hydroperoxides in the soybean oil and oleic

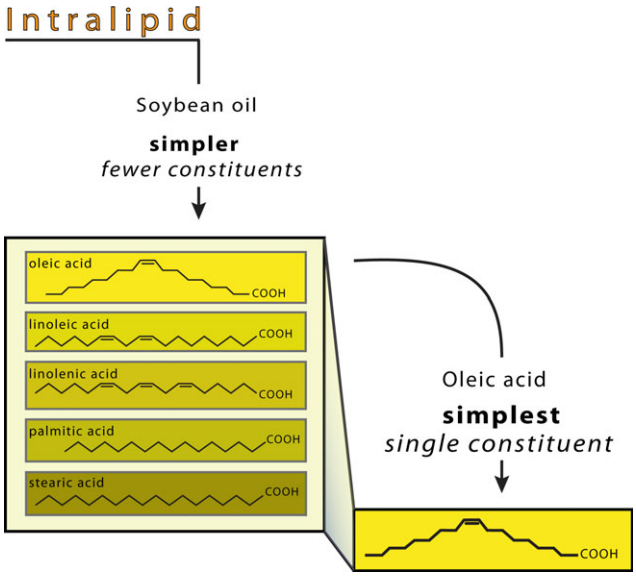

Figure 6. Schematic image showing simpler "model" reactions (soybean oil and oleic acid) in place of Intralipid.

acid photooxidation samples were observed in CD_3OD, based on integration of the allylic hydrogens of the "ene" products in the mixtures. The "ene" reaction is a fingerprint for the presence of $^1O_2$. The oleic acid hydroperoxide percent yield derived from ^1H NMR is within error bounds (11 ± 1%) of that observed by trapping with phosphine **2** (10 ± 1%) in CD_3OD (Figures S1 and S2). Thus, the trapping findings from ^{31}P NMR are consistent with ^1H NMR data.

Mechanistic considerations

A mechanistic summary is shown here. It indicates that in the series of phosphines, **2** is the most suitable trapping agent of Intralipid peroxides.

(1) *Trapping and reactivity.* The results demonstrate that phosphine **2** is the best in the series due to its moderate reactivity. The time required to trap peroxides with phosphines varies from moderate (**2**) to high (**3**) to low (**1**) (Table 2 and Fig. 9). The phosphine stability pattern clearly indicates that the fewer the cyclohexyl groups, the more stable the phosphine. sSPhos **1** is capable of trapping the peroxy

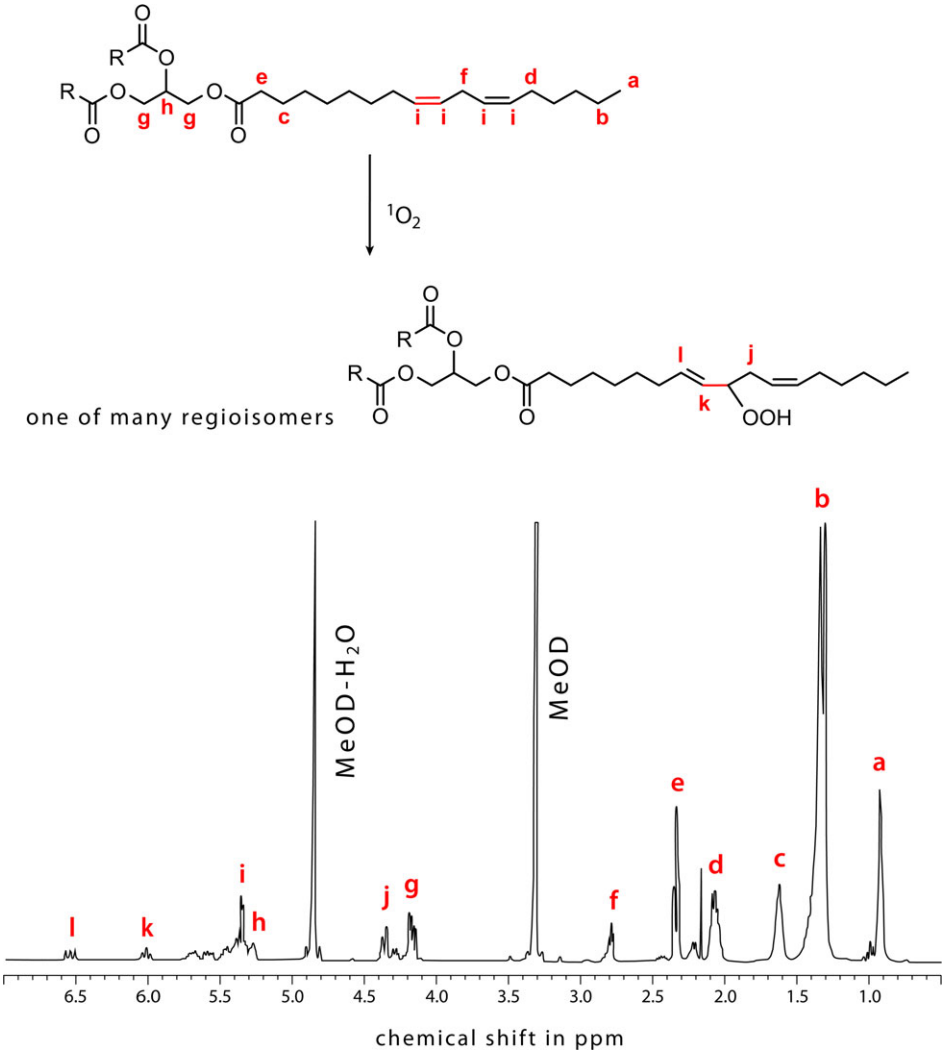

Figure 7. ^1H NMR spectrum of soybean oil after photooxidation: formation of hydroperoxides of a triglyceride linolenic acid constituent in CD_3OD. This is a simpler reaction than Intralipid because it contains fewer constituents.

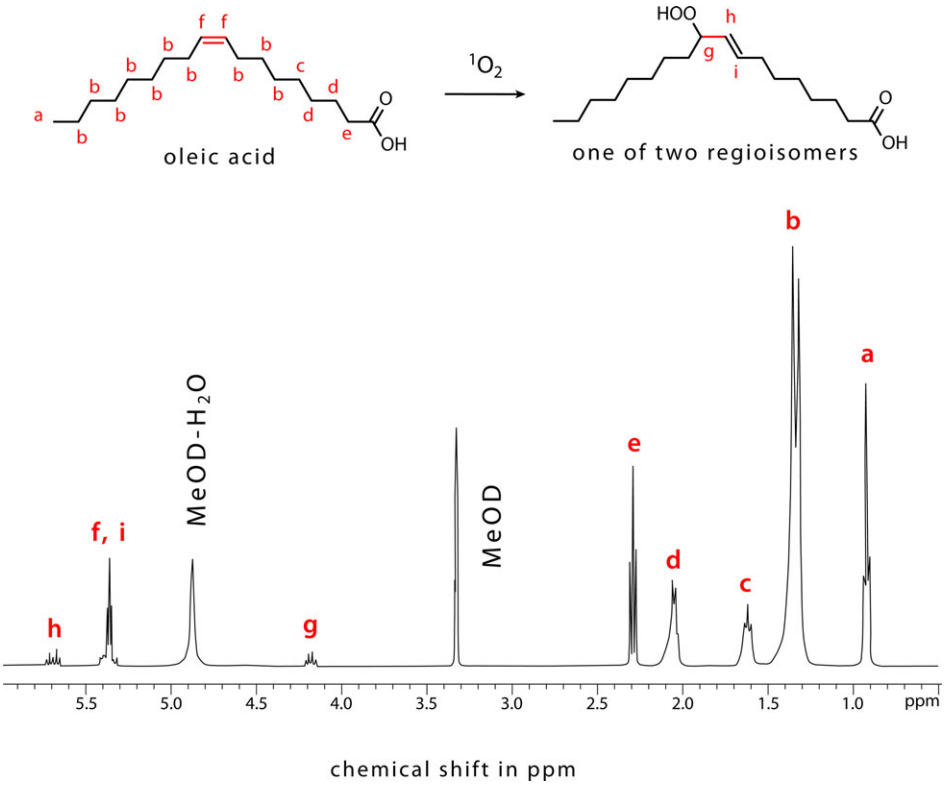

Figure 8. ^{1}H NMR spectrum of oleic acid: formation of hydroperoxides after photooxidation in CD_3OD. This reaction has only two constituents.

Table 2. Phosphine solubility, stability and reactivity

Phosphine trapping agent	Solubility	Stability	Reactivity
1	Insoluble in water at room temperature, soluble on heating to 40°C 100 mg L^{-1}*	Commercial sample contained 7% oxide impurity, quality of sample rapidly decreased over time	Reacts with hydroperoxides instantly
2	Water soluble on slightly warming 100 mg L^{-1}*	Commercial sample had no oxide impurity	Reacts with hydroperoxides within minutes
3	Water soluble at room temperature 100 mg L^{-1}*	Commercial sample contained 5% oxide impurity	After 12 h, reaction with hydroperoxides was incomplete
4	Insoluble in water, soluble in organic solvents 50 mg mL^{-1}, $CHCl_3$†	Commercial sample had no oxide impurity	Reacts with hydroperoxides instantly

*Observed in this study. †Reported in compound specification sheet (Aldrich).

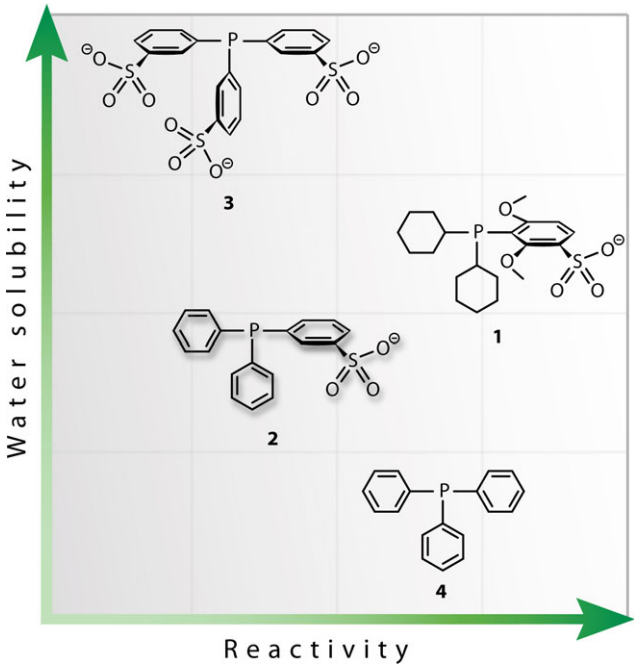

Figure 9. Reactivity vs. water solubility of phosphines: The phosphines are, with the exception of **4**, water soluble.

intermediates, but also undergoes air oxidation, thus when used to trap peroxides required a subtraction to account for the extra **1** oxide. Phosphine **3** is a poor trapping agent due to an electronically deactivated phosphorus site. Experiments showed that the percent yield of **3** oxide was poor due to the low reactivity of **3**.

(2) *Water solubility.* Sulfonate groups are water-solubilizing groups, but also electron-withdrawing groups. Therefore, the introduction of a sulfonate group increases the water solubility of the phosphine, but decreases the nucleophilicity and

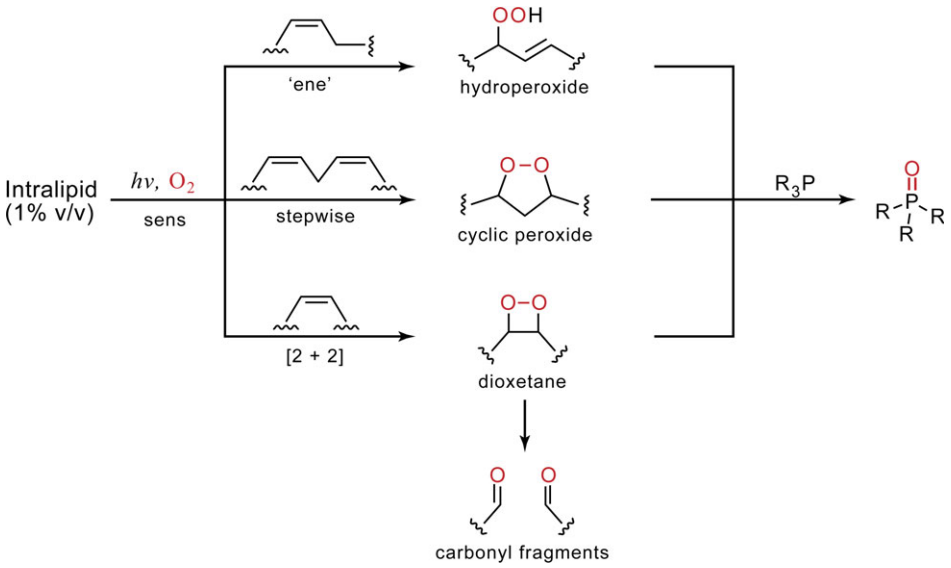

Figure 10. Proposed mechanism of peroxide trapping by phosphines.

oxophilicity. Phosphine **3** is relatively unreactive to Intralipid peroxides because of its three sulfonate groups, while phosphine **4** is relatively unreactive to Intralipid peroxides because of its water insolubility.

(3) *Peroxide type.* The ^{1}H NMR data indicate that hydroperoxides are the major products in the Intralipid photooxidation reaction (Fig. 10). Dioxetanes can also be formed, but are unstable and consequently decompose to carbonyl fragments during the reaction. We have not quantitated dioxetanes that would likely decompose prior to the phosphine trapping. Peroxides can also be formed by type I reactions, such as those formed from unconjugated dienes and related compounds (60–62). A stepwise pathway accounts for the decomposition of the peroxides, where the phosphines react with peroxides to mainly produce alcohol products. The production of peroxides is consistent with previous literature on the reactions of $^{1}O_2$ with unsaturated lipids and alkene compounds (63–66). Many $^{1}O_2$ reactions with lipids have already been published, but we feel that those do not reduce the importance of our study.

Overall, the data show the requirement for a balance of nucleophilicity and water solubility in the phosphine.

A Hamlet-like question on the Intralipid peroxides came to mind: *To quantitate or not to quantitate?* Our Intralipid photooxidation shows the postphotoreaction trapping with phosphines to remove the formed peroxides. We suggest that this photooxidation susceptibility becomes increasingly important for photooxidatively aged Intralipid samples from patients due to the leakage of sensitizer into the pleural cavity. Intralipid hydroperoxides may have an unexpected toxic side, including excited states arising in peroxy thermal decomposition processes.

While ^{18}O and ^{15}N labeling (67–72) have been exploited to elucidate mechanistic aspects of PDT, the natural ^{31}P abundance of phosphine traps has not been explored in depth yet, as done here in a PDT relevant project.

CONCLUSION

Phosphines **1**–**4** are usually reserved for use in organic and inorganic synthesis (31–36,48). Here, **1** and **2**, but not **3** and **4**, were shown to be efficient trapping agents for peroxides in postphotooxidation/photoreactions of Intralipid. Our phosphine trapping and monitoring by the ^{31}P NMR method are effective in quantifying the peroxides, even though the production of $^{1}O_2$ is not detected during the light delivery for PDT. For example, a linear dependence of Intralipid peroxides on light fluence was observed. The photooxidation yields quantitated by ^{31}P NMR of the phosphine traps are supported by the direct ^{1}H NMR detection of oleic acid hydroperoxides. One virtue of phosphine trapping technique is that peroxides are detected in the constituents of Intralipid in protio not deutero media.

Future directions in this research include the quantitation of sensitizer concentration in the pleural cavity after the PDT using phosphine trapping with a suitable phosphine trap and ^{31}P NMR spectroscopy. The use of a higher field NMR would further facilitate the phosphine trapping method in biological samples. The use of Intralipid mixed with blood and saline solution as a model for plasma is currently being studied to assess the effect on $^{1}O_2$ uptake due to blood contamination. It remains to be seen whether these peroxy intermediates play a significant role in Intralipid phototoxicity. It would be interesting to understand the biological activity of photooxidized Intralipid samples.

Acknowledgements—P.P.M., C.O.C., A.K. and A.G. acknowledge the support from the National Science Foundation (CHE-1464975). M.M.K., T.C.Z. and T.M.B. acknowledge the support from the National Institutes of Health (NIH) R01 CA154562 and/or P01 CA87971. A.G. acknowledges the support from a Tow Professorship at Brooklyn College. We thank Niluksha Walalawela for comments and Leda Lee for the graphic arts work.

SUPPORTING INFORMATION

Additional Supporting Information may be found in the online version of this article:

Figure S1. ^{1}H NMR spectrum of oleic acid hydroperoxides after photooxidation in CD_3OD.

Figure S2. ^{31}P NMR spectrum of phosphine **2** and its oxide after photooxidation of oleic acid and trapping in CD_3OD.

Figure S3. ^{31}P NMR spectrum of phosphine **2** and its oxide after photooxidation of Intralipid and trapping in D_2O.

Figure S4. ^{31}P NMR spectrum of phosphine **3** and its oxide after photooxidation of Intralipid and trapping in D_2O.

REFERENCES

1. Zhu, T. C., M. M. Kim, X. Liang, J. C. Finlay and T. M. Busch (2015) In-vivo singlet oxygen threshold doses for PDT. *Photon. Lasers Med.* **4**, 59–71.
2. Sandell, J. L. and T. C. Zhu (2011) A review of in-vivo optical properties of human tissues and its impact on PDT. *J. Biophotonics* **4**, 773–787.
3. Zhu, T. C. and C. Jarod (2006) Finlay prostate PDT dosimetry. *Photodiagn. Photodyn. Ther.* **3**, 234–246.
4. Penjweini, R., M. Kim and T. C. Zhu (2016) Finite element-based deformable image registration of lung and heart. *Med. Phys.* **43**, 3398–3398.
5. Baran, T. M., M. C. Fenn and T. H. Foster (2013) Determination of optical properties by interstitial white light spectroscopy using a custom fiber optic probe. *J. Biomed. Opt.* **18**, 107007.
6. Dimofte, A., J. C. Finlay and T. C. Zhu (2005) A method for determination of the absorption and scattering properties interstitially in turbid media. *Phys. Med. Biol.* **50**, 2291–2311.
7. Hu, X.-H., Y. Feng, J. Q. Lu, R. R. Allison, R. E. Cuenca, G. H. Downie and C. H. Sibata (2005) Modeling of a type II Photofrin-mediated photodynamic therapy process in a heterogeneous tissue phantom. *Photochem. Photobiol.* **81**, 1460–1468.
8. Wagnières, G., S. Cheng, M. Zellweger, N. Utke, D. Braichotte, J. P. Ballini and H. Van den Bergh (1997) An optical phantom with tissue-like properties in the visible for use in PDT and fluorescence spectroscopy. *Phys. Med. Biol.* **42**, 1415–1426.
9. Flock, S. T., S. J. Jacques, B. C. Wilson, W. M. Star and M. J. C. Van Gemert (1992) Optical properties of intralipid: A phantom medium for light propagation studies. *Lasers Surg. Med.* **12**, 516–519.
10. Allardice, J. T., A. M. Abulafi, D. G. Webb and N. S. Williams (1992) Standardization of intralipid for light scattering in clinical photodynamic therapy. *Lasers Med. Sci.* **7**, 461–465.
11. Girotti, A. W. and W. Korytowski (2016) Reactions of singlet oxygen with membrane lipids: lipid hydroperoxide generation, translocation, reductive turnover, and signaling activity. *Comprehens. Ser. Photochem. Photobiol. Sci.* **13**(Singlet Oxygen, Vol. 1), 409–430.
12. Girotti, A. W. and W. Korytowski (2016) Reactions of singlet oxygen with membrane lipids: Lipid hydroperoxide generation, translocation, reductive turnover, and signaling activity. In *Singlet Oxygen: Applications in Biosciences and Nanosciences*, Vol. **1** (Edited by S. Nonell and C. Flors), pp. 409–430. Royal Society of Chemistry, Cambridge, UK.
13. Miyamoto, S., G. R. Martinez, G. E. Ronsein, E. F. Marques, F. M. Prado, K. R. Prieto, M. H. G. Medeiros, J. Cadet and P. Di Mascio (2016) [^{18}O]-labeled singlet molecular oxygen: Chemical generation and trapping as a tool for mechanistic studies. *Comprehens Ser Photochem Photobiol Sci* **14**(Singlet Oxygen, Vol. 2), 135–150.
14. Di Mascio, P., S. Miyamoto, M. H. G. Medeiros, G. R. Martinez and J. Cadet (2014) [^{18}O]-peroxides: Synthesis and biological applications. In *Chemistry of Peroxides*, Vol. **3 (Pt. 2)** (Edited by S. Patai and Z. Rappoport), pp. 769–804. Wiley, Chichester, UK.
15. Itri, R., H. C. Junqueira, O. Mertins and M. S. Baptista (2014) Membrane changes under oxidative stress: The impact of oxidized lipids. *Biophys. Rev.* **6**, 47–61.
16. Ytzhak, S. and B. Ehrenberg (2014) The effect of photodynamic action on leakage of ions through liposomal membranes that contain oxidatively modified lipids. *Photochem. Photobiol.* **90**, 796–800.
17. Bacellar, I. O. L., C. Pavani, E. M. Sales, R. Itri, M. Wainwright and M. S. Baptista (2014) Membrane damage efficiency of phenothiazinium photosensitizers. *Photochem. Photobiol.* **90**, 801–813.
18. Kyagova, A., A. Potapenko, M. Möller, H. Stopper and W. Adam (2014) Photohemolysis sensitized by the furocoumarin derivative alloimperatorin and its hydroperoxide photooxidation product. *Photochem. Photobiol.* **90**, 162–170.
19. Korytowski, W., J. C. Schmitt and A. W. Girotti (2010) Surprising inability of singlet oxygen-generated 6-hydroperoxycholesterol to induce damaging free radical lipid peroxidation in cell membranes. *Photochem. Photobiol.* **86**, 747–751.
20. Greer, A. (2007) Organic chemistry: Molecular crosstalk. *Nature* **447**, 273–274.
21. Orfanopoulos, M., G. C. Vougioukalakis and M. Stratakis (2006) Selective formation of allylic hydroperoxides via singlet oxygenene reaction. In *Chemistry of Peroxides*, Vol. **2(Pt. 2)** (Edited by Z. Rappoport), pp. 831–898. Wiley, Chichester, UK.
22. Niziolek, M., W. Korytowski and A. W. Girotti (2005) Self-sensitized photodegradation of membrane-bound protoporphyrin mediated by chain lipid peroxidation: Inhibition by nitric oxide with sustained singlet oxygen damage. *Photochem. Photobiol.* **81**, 299–305.
23. Thompson, D. H., H. D. Inerowicz, J. Grove and T. Sarna (2003) Structural characterization of plasmenylcholine photooxidation products. *Photochem. Photobiol.* **78**, 323–330.
24. Min, D. B. and J. M. Boff (2002) Chemistry and reaction of singlet oxygen in foods. *Compr. Rev. Food Sci. Food Saf.* **1**, 58–72.
25. Stratakis, M. and M. Orfanopoulos (2000) Regioselectivity in the ene reaction of singlet oxygen with alkenes. *Tetrahedron* **56**, 1595–1615.
26. Foote, C. S. and E. L. Clennan (1995) Properties and reactions of singlet dioxygen. In *Active Oxygen in Chemistry*, Vol. **2** (Edited by C. S. Foote, J. S. Valentine, J. F. Liebman and A. Greenberg), pp. 105–140. Chapman & Hall, New York.
27. Gemmell, N. R., A. McCarthy, M. M. Kim, I. Veilleux, T. C. Zhu, G. S. Buller, B. C. Wilson and R. H. Hadfield (2017) A compact fiber-optic probe-based singlet oxygen luminescence detection system. *J. Biophotonics* **10**, 320–326.
28. Wang, H.-W., T. C. Zhu, M. E. Putt, M. Solonenko, J. Metz, A. Dimofte, J. Miles, D. L. Fraker, E. Glatstein, S. M. Hahn and A. G. Yodh (2005) Broadband reflectance measurements of light penetration, blood oxygenation, hemoglobin concentration, and drug concentration in human interperitoneal tissues before and after photodynamic therapy. *J. Biomed. Opt.* **10**, 014004.
29. Friedberg, J. S., M. J. Culligan, R. Mick, J. Stevenson, S. M. Hahn, D. Sterman, S. Punekar, E. Glatstein and K. Cengel (2012) Radical pleurectomy and intraoperative photodynamic therapy for malignant pleural mesothelioma. *Ann. Thorac. Surg.* **93**, 1658–1667.
30. Friedberg, J. S., C. B. Simone, M. J. Culligan, A. R. Barsky, A. Doucette, S. McNulty, S. M. Hahn, E. Alley, D. H. Sterman, E. Glatstein and K. A. Cengel (2017) Extended pleurectomy-decortication–based treatment for advanced stage epithelial mesothelioma yielding a median survival of nearly three years. *Ann. Thorac. Surg.* **103**, 912–919.
31. Jiang, H., T. Jia, M. Zhang and P. J. Walsh (2016) Palladium-catalyzed arylation of aryl sulfenate anions with aryl bromides under mild conditions: Synthesis of diaryl sulfoxides. *Org. Lett.* **18**, 972–975.
32. Molander, G. A., D. Ryu, M. Hosseini-Sarvari, R. Devulapally and D. G. Seapy (2013) Suzuki-Miyaura cross-coupling of potassium trifluoro(N-methylheteroaryl)borates with aryl and heteroaryl halides. *J. Org. Chem.* **78**, 6648–6656.
33. Jung, H. H., A. W. Buesking and J. A. Ellman (2011) Highly functional group compatible Rh-catalyzed addition of arylboroxines to activated *N-tert*-butanesulfinyl ketimines. *Org. Lett.* **13**, 3912–3915.
34. Gulyás, H., J. Benet-Buchholz, E. C. Escudero-Adan, Z. Freixa and P. W. N. M. van Leeuwen (2007) Ionic interaction as a powerful driving force for the formation of heterobidentate assembly ligands. *Chem. Eur. J.* **13**, 3424–3430.
35. Mauger, C. C. and G. A. Mignani (2006) Synthetic applications of Buchwald's phosphines in palladium-catalyzed aromatic-bond-forming reactions. *Aldrichimica Acta* **39**, 17–24.
36. Schlummer, B. and U. Scholz (2004) Palladium-catalyzed C–N and C–O coupling: A practical guide from an industrial vantage point. *Adv. Synth. Catal.* **346**, 1599–1626.
37. Bonesi, S. M., S. Protti and A. Albini (2016) Reactive oxygen species (ROS)-vs peroxyl-mediated photosensitized oxidation of triphenylphosphine: A comparative study. *J. Org. Chem.* **81**, 11678–11685.
38. Yasui, S., M. R. Badal, S. Kobayashi and M. Mishima (2014) Combination of LFP-TRIR spectroscopy and DFT computation as a tool

to determine the intermediate during the photooxidation of triarylphosphine. *J. Phys. Org. Chem.* **27**, 967–972.
39. Zhang, D., J. Celaje, A. Agua, C. Doan, T. Stewart, R. Bau and M. Selke (2010) Photooxidation of mixed aryl and biaryl phosphines. *Org. Lett.* **10**, 3100–3103.
40. Harris, J. R., M. T. Haynes II, A. M. Thomas and K. A. Woerpel (2010) Phosphine-catalyzed reductions of alkyl silyl peroxides by titanium hydride reducing agents: Development of the method and mechanistic investigations. *J. Org. Chem.* **75**, 5083–5091.
41. Nahm, K. (2009) A theoretical study on the reaction of phosphadioxiranes and thiadioxiranes; disproportionation versus epoxidation. *Bull. Korean Chem. Soc.* **30**, 2217–2222.
42. Reva, I., L. Lapinski and M. J. Nowak (2008) Photoinduced oxidation of triphenylphosphine isolated in a low-temperature oxygen matrix. *Chem. Phys. Lett.* **467**, 97–100.
43. Ho, D. G., R. Gao, J. Celaje, H.-Y. Chung and M. Selke (2003) Phosphadioxirane: A peroxide from an ortho-substituted arylphosphine and singlet dioxygen. *Science* **302**, 259–262.
44. Clennan, E. L., M. F. Chen and G. Xu (1996) New potent trapping agents for the peroxidic intermediates formed in the reactions of singlet oxygen. *Tetrahedron Lett.* **37**, 2911–2914.
45. Clennan, E. L. and P. C. Heah (1984) Bicyclic dioxaphosphoranes 4. A kinetic investigation of the reactions of trivalent phosphorus compounds with bicyclic endoperoxides. *J. Org. Chem.* **49**, 2284–2286.
46. Clennan, E. L. and P. C. Heah (1981) Interaction of triphenylphosphine with 2,3-dioxabicyclo[2.2.1]heptane. *J. Org. Chem.* **46**, 4105–4107.
47. Bartlett, P. D., A. L. Baumstark and M. E. Landis (1973) Insertion reaction of triphenylphosphine with tetramethyl-1,2-dioxetane. Deoxygenation of a dioxetane to an epoxide. *J. Am. Chem. Soc.* **95**, 6486–6487.
48. Elie, B. T., C. Levine, I. Ubarretxena-Belandia, A. Varela, R. Aguilera, R. Ovalle and M. Contel (2009) Water-soluble phosphane-gold (I) complexes. Applications as recyclable catalysts in a three-component coupling reaction and as anticancer and antimicrobial agents. *Eur. J. Inorg. Chem.* **23**, 3421–3430.
49. Zhu, T. C., J. C. Finlay, A. Dimofte and S. M. Hahn (2003) Light dosimetry at tissue surface for small circular fields. *Proc. SPIE* **4952**, 56–67.
50. Jacques, S. L. (1998) Light distributions from point, line, and plane sources for photochemical reactions and fluorescence in turbid biological tissues. *Photochem. Photobiol.* **67**, 23–32.
51. Fleming, J. T. and L. J. Higham (2015) Primary phosphine chemistry. *Coord. Chem. Rev.* **297–298**, 127–145.
52. Hiney, R. M., A. Ficks, H. Muller-Bunz, D. G. Gilheany and L. J. Higham (2011) Air-stable chiral primary phosphines part (i) synthesis, stability and applications. *Organomet. Chem.* **37**, 27–45.
53. Cai, F., N. D. Thangada, E. Pan and J. M. Ready (2013) On the rapid oxidation of allene-containing phosphines. *Organometallics* **32**, 5619–5622.
54. Frausto, F. and S. W. Thomas (2017) Ratiometric singlet oxygen detection in water using acene-doped conjugated polymer nanoparticles. *ACS Appl. Mater. Interfaces.* **9**, 15768–15775.
55. Machacek, M., A. Jedlickova, T. Simunek, J. Demuth, P. Cermak, L. Hruba, V. Novakova, M. Vavreckova, P. Zimcik and P. Kubat (2016) Tetra(3,4-pyrido)porphyrazines caught in the cationic cage: Toward Nanomolar active photosensitizers. *J. Med. Chem.* **59**, 9443–9456.
56. Park, S. L., R. Justiniano, J. D. Williams, C. M. Cabello, S. Qiao and G. T. Wondrak (2015) The tryptophan-derived endogenous aryl hydrocarbon receptor ligand 6-formylindolo[3,2-b]carbazole is a nanomolar UVA photosensitizer in epidermal keratinocytes. *J. Invest. Dermatol.* **135**, 1649–1658.
57. Syed, D. N. and H. Mukhtar (2015) FICZ: A messenger of light in human skin. *J. Invest. Dermatol.* **135**, 1478–1481.
58. Arenas, Y., S. Monro, G. Shi, A. Mandel, S. McFarland and L. Lilge (2013) Photodynamic inactivation of *Staphylococcus aureus* and methicillin-resistant *Staphylococcus aureus* with Ru(II)-based type I/type II photosenstizers. *Photodiagn. Photodyn. Ther.* **10**, 615–625.
59. Boch, R., A. J. Canaan, A. Cho, D. D. Dolphin, L. Hong, A. K. Jain, J. R. North, A. M. Richter, C. Smits and E. D. Sternberg (2006) Cellular and antitumor activity of a new diethylene glycol benzoporphyrin derivative (lemuteporfin). *Photochem. Photobiol.* **82**, 219–224.
60. Cadet, J., C. Decarroz, S. Y. Wang and W. R. Midden (1983) Mechanisms and products of photosensitized degradation of nucleic acids and related model compounds. *Isr. J. Chem.* **23**, 420–429.
61. Ghogare, A. A. and A. Greer (2016) Using singlet oxygen to synthesize natural products and drugs. *Chem. Rev.* **116**, 9994–10034.
62. Baptista, M. S., J. Cadet, P. Di Mascio, A. A. Ghogare, A. Greer, M. R. Hamblin, C. Lorente, S. C. Nunez, M. S. Ribeiro, A. H. Thomas, M. Vignoni and T. M. Yoshimura (2017) Type I and II photosensitized oxidation reactions: Guidelines and mechanistic pathways. *Photochem. Photobiol.* **93**, 912–919.
63. Di Mascio, P., G. R. Martinez, S. Miyamoto, G. E. Ronsein, M. H. G. Medeiros and J. Cadet (2016) Singlet molecular oxygen: Düsseldorf-São Paulo, the Brazilian connection. *Arch. Biochem. Biophys.* **595**, 161–175.
64. Di Masio, P., L. H. Catalani and E. J. H. Bechara (1992) Are dioxetanes chemiluminescent intermediates in lipoperoxidation?. *Free Rad. Biol. Med.* **12**, 471–478.
65. Ghorai, P. and P. H. Dussault (2009) A new peroxide fragmentation: Efficient chemical generation of $^1O_2$ in organic media. *Org. Lett.* **11**, 4572–4575.
66. Dussault, P. H. (1995) The peroxide changes everything. *Synlett*, **10**, 997–1003.
67. Hsieh, Y. J., K. Y. Chien, S. Y. Lin, S. Sabu, R. M. Hsu, L. M. Chi, P. C. Lyu and J. S. Yu (2012) Photofrin binds to procaspase-3 and mediates photodynamic treatment-triggered methionine oxidation and inactivation of procaspase-3. *Cell Death Dis.* **3**, e347/1–e347/11.
68. Diller, A., E. Roy, P. Gast, H. J. van Gorkom, H. J. M. de Groot, C. Glaubitz, G. Jeschke, J. Matysik and A. Alia (2007) ^{15}N photochemically induced dynamic nuclear polarization magic-angle spinning NMR analysis of the electron donor of photosystem II. *Proc. Natl Acad. Sci. USA* **104**, 12767–12771.
69. Kang, P. and C. S. Foote (2002) Photosensitized oxidation of ^{13}C, ^{15}N-labeled imidazole derivatives. *J. Am. Chem. Soc.* **124**, 9629–9638.
70. Matter, B., D. Malejka-Giganti, A. S. Csallany and N. Tretyakova (2006) Quantitative analysis of the oxidative DNA lesion, 2,2-diamino-4-(2-deoxy-*β*-D-erythro-pentofuranosyl) amino]-5(2*H*)-oxazolone (oxazolone), in vitro and in vivo by isotope dilution-capillary HPLC-ESI-MS/MS. *Nucleic Acids Res.* **34**, 5449–5460.
71. Kruppa, A. I., M. B. Taraban, N. E. Polyakov, T. V. Leshina, V. Lūsis, D. Muceniece and G. Duburs (1993) The mechanisms of the oxidation of NADH analogues 2. *N*-Methyl-substituted 1,4-dihydropyridines. *J. Photochem. Photobiol. A: Chem.* **73**, 159–163.
72. Diwu, Z. and J. W. Lown (1993) Photosensitization with anticancer agents 16. The photo-oxidation of hypocrellin A. A mechanism study using ^{18}O labelling. *J. Photochem. Photobiol. B: Biol.* **18**, 145–154.